Scientific Papers. Series E. Land Reclamation, Earth Observation & Surveying, Environmental Engineering. Vol. XV, 2026
Print ISSN 2285-6064, CD-ROM ISSN 2285-6072, Online ISSN 2393-5138, ISSN-L 2285-6064

ASSESSING WINTER MICROCLIMATES AND URBAN-RURAL THERMAL DIFFERENCES: A MOBILE MONITORING PILOT STUDY IN SOUTH-EASTERN ROMANIA

Sorin FRĂSINA[1, 2], Adrian ROȘU[1, 3], Bogdan ROȘU[1, 3], Maxim ARSENI[1, 3], Daniel-Eduard CONSTANTIN[1, 3], Mădălin CRISTEA[1], Lucian SFÎCĂ[4], Cătălina ITICESCU[1, 2], Silvia DRAGAN[5]

[1]"Dunarea de Jos" University of Galati, Faculty of Sciences and Environment, Department of Chemistry, Physics and Environment, 111 Domneasca Street, Galati, Romania
[2]"Dunarea de Jos" University of Galati, Faculty of Engineering, 111 Domneasca Street, Galati, Romania
[3]"Dunarea de Jos" University of Galati, REXDAN Research Infrastructure, 98 George Cosbuc Street, Galati, Romania
[4]"Alexandru Ioan Cuza" University, Faculty of Geography and Geology, Department of Geography, 20A Carol I Street, 700506, Iași, Romania
[5]EnviroEcoSmart S.R.L., Tecuci Street no. 189, Galati, Romania

Corresponding author email: adrian.rosu@ugal.ro

Abstract

Rapid urbanization alters the thermal environment of cities, leading to the urban heat island effect. Because fixed meteorological stations cannot adequately capture high-resolution intra-urban microclimate variability, mobile monitoring has emerged as an essential complementary approach. This exploratory pilot study evaluated the utility of high-resolution mobile measurements for capturing winter microclimatic signatures along a regional transect in South-Eastern Romania, encompassing small and medium-sized urban hubs. Data were collected on February 10, 2026, under stable atmospheric conditions, using a vehicle-mounted weather station equipped with a radiation error correction system. To ensure scientific integrity, a three-stage quality control and normalization workflow was implemented. This included excluding data points recorded at speeds below 10 km/h to prevent thermal contamination, applying an altitude correction to a common reference level, and performing a time-drift correction based on official meteorological stations to isolate the spatial microclimatic signal. The spatially dense mobile data effectively identified critical thermal gradients and specific urban footprints. In conclusion, the study highlighted the value of mobile monitoring as a viable tool for assessing microclimatic spatial variations, providing detailed insights into urban-rural thermal contrasts during the cold season.

Key words: *altitude correction, Meteotracker, mobile measurements, temperature gradient, urban microclimate, urban-rural contrast.*

INTRODUCTION

Rapid urbanization and significant land-use modifications have profoundly altered the thermal environment of cities, leading to the well-documented Urban Heat Island (UHI) effect (Oke, 1982). The canopy layer (CUHI), characterized by higher air temperatures in urbanized areas compared to their rural surroundings, poses severe challenges to urban variability of urban microclimates is critical for developing effective mitigation and adaptation strategies.

Traditionally, the assessment of urban thermal environments has relied on fixed meteorological sustainability, energy consumption, and human thermal comfort (Santamouris, 2015; Li et al., 2024). Urban overheating may significantly reduce climate resilience and increase thermal exposure risks for urban populations under future climate scenarios (Emmanuel & Krüger, 2012). As extreme weather events and heatwaves become more frequent, understanding the fine-scale spatial and temporal

stations. While these stations provide reliable, long-term synoptic data, their sparse spatial distribution makes them inadequate for capturing high-resolution intra-urban microclimate variability and the sharp

temperature gradients at urban-rural boundaries (Stewart & Oke, 2012; Martinez-Soto et al., 2025). Furthermore, previous studies demonstrated that urban-rural thermal contrasts are strongly influenced by land use and surface characteristics (Hart & Sailor, 2009). To address this spatial data gap, mobile monitoring has emerged as a robust complementary approach (Romero Rodríguez et al., 2020; Kousis et al., 2021; 2022; Martinez-Soto et al., 2025). Vehicle-based mobile measurements act as itinerant sensors, enabling the continuous recording of meteorological parameters across diverse land-cover types and topographical profiles within a short timeframe. Such approaches have been successfully applied to investigate fine-scale canopy layer thermal variability and spatial urban heat patterns (Brandsma & Wolters, 2012). Urban morphology, vegetation cover, and street geometry may substantially modify local thermal conditions and microclimatic variability at neighborhood scale (Middel et al., 2014).

Despite its advantages, mobile monitoring introduces challenges, primarily the "radiative error" caused by solar radiation heating the sensors at varying speeds. Recent technological advancements have led to the development of compact mobile sensors, such as the MeteoTracker (Barbano et al., 2024), which deploys a patented dual-sensor Radiation Error Correction System (RECS) (Jurato, 2020; MeteoTracker, 2025). This system ensures high-accuracy thermal measurements even under strong solar exposure, making it highly suitable for high-resolution investigations.

In Romania, recent studies have begun to map the UHI in major cities like Iași (Sfîcă et al., 2018; 2023), yet multi-city comparative transects investigating the thermal gradients between smaller urban hubs and rural plains remain scarce (Ichim et al., 2024). This is particularly true for winter conditions, which are often overlooked in favor of summer stress studies (Crétat et al., 2024), despite the important role of nighttime urban thermal retention under stable atmospheric conditions (Eliasson, 1996).

Therefore, this study is designed as an exploratory pilot study aiming to evaluate the interpretative value of high-resolution mobile surveys during a single winter day in South-Eastern Romania. The measurement date, 10 February 2026, was selected because it was characterized by stable winter atmospheric conditions, weak wind, absence of precipitation, and limited synoptic variability, which are favorable for identifying spatial thermal contrasts between different land-use environments. By utilizing the MeteoTracker sensor on a complex transect intersecting Focșani, Râmnicu Sărat, Buzău, Ianca, Brăila, and Galați, this paper explores the potential of spatially dense mobile data to capture fine-scale microclimatic signatures (Chàfer et al., 2022). The aim of the study was not to provide a climatological assessment of the winter urban heat island, but to test whether mobile monitoring can identify localized thermal gradients and urban footprints during suitable atmospheric conditions. While recognizing the temporal limitations of a single-day measurement, the study emphasizes the spatial richness of the data as a tool for identifying critical thermal gradients in Urban, Rural, and Road environments. In addition, high-resolution spatial observations provide valuable support for understanding local thermal variability and improving urban climate assessment methodologies (Voogt & Oke, 2003).

Satellite-derived Land Surface Temperature (LST) may complement mobile air temperature measurements by describing surface thermal patterns. However, LST refers to the land surface, while this study analyzes near-surface air temperature measured at road level. For this reason, Landsat-derived LST was not included in the present quantitative analysis, but it should be considered in future studies.

MATERIALS AND METHODS

Study Area and Meteorological Context

The study area spans a complex regional transect in South-Eastern Romania, covering a diverse topographical and land-use profile. The mobile survey originated in the rural area of Slobozia Conachi (Galați County) and intersected several urban hubs of varying sizes: Focșani, Râmnicu Sărat, Buzău, Ianca, Brăila, and Galați (see Figure 2). Mobile measurements are recognized for their ability to capture high-resolution spatial variability that fixed station networks often miss

(Kousis et al., 2022; Martinez-Soto et al., 2025). To establish a synoptic baseline, air temperature data from the official National Meteorological Administration (ANM) stations WMO-15310 (Galați) and WMO-15350 (Buzău) were used to compensate for the temporal drift of the mobile measurements during the transect survey (*Meteo Buzău, 10.02.2026*, 2026; *Meteo Galaţi, 10.02.2026*, 2026). The reference meteorological data consisted of hourly air temperature observations recorded at the two WMO stations during the mobile survey interval. These hourly values were linearly interpolated to the timestamp of each mobile measurement and then averaged in order to obtain a regional temperature trend used for temporal normalization. The Galați and Buzău stations were selected because they were the most relevant official meteorological stations located near the main monitored sectors of the transects and provided representative information for the regional air mass evolution during the survey. Additional stations were not included because they were either farther from the monitored routes or less representative for the spatial domain covered by the mobile measurements. Therefore, the two-station approach was used only for correcting the temporal drift of the mobile observations, not for replacing the high-resolution spatial information provided by the mobile survey.

Figure 1 illustrates the air temperature evolution recorded at the Galați and Buzău WMO stations on 10 February 2026, highlighting stable winter atmospheric conditions and a gradual daytime warming trend during the survey period.

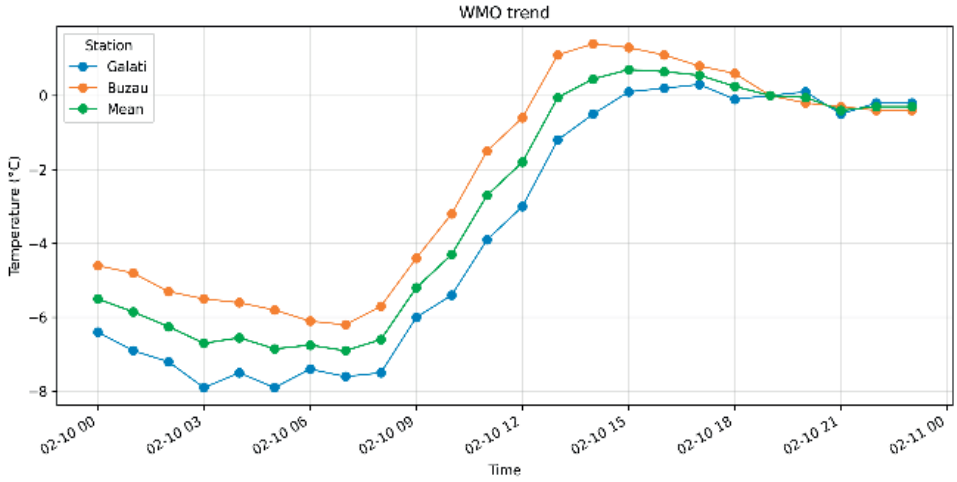


Figure 1.Temporal evolution of air temperature recorded at the WMO reference stations during the mobile survey. The blue line represents the Galați station (WMO-15310), the orange line represents the Buzău station (WMO-15350), and the green line indicates the mean regional temperature trend used for temporal normalization of the mobile measurements (Meteo Buzău, 10.02.2026, 2026; Meteo Galaţi, 10.02.2026, 2026)

These hourly reference data provided the regional synoptic background and were used for the temporal normalization of the mobile measurements. The hourly observations were interpolated to the exact time of each mobile record, and the mean trend of the two WMO stations was used to correct the mobile temperature values for the natural daytime thermal evolution.

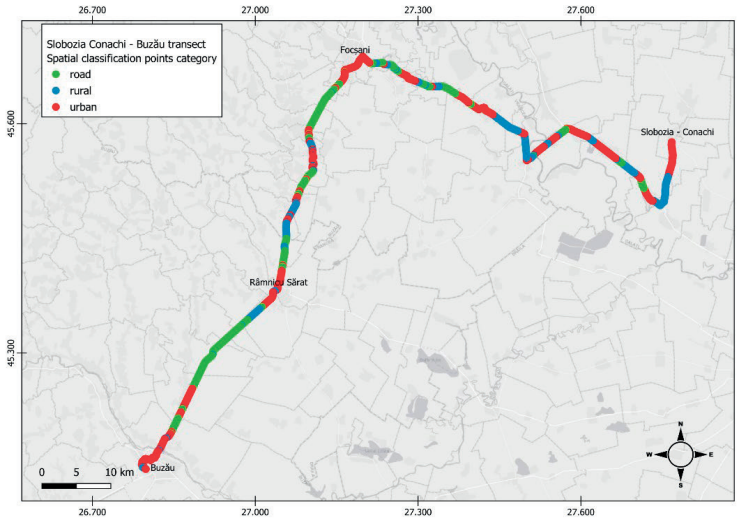
The measurements were conducted on 10 February 2026 in eastern Romania along two regional mobile transects between Slobozia Conachi-Buzău and Buzău-Galați (Figure 2), under stable winter atmospheric conditions favorable for the identification of microclimatic gradients and urban heat island (UHI) signatures (Crétat et al., 2024; Li et al., 2024). Data extracted from the official WMO stations in Galați and Buzău confirmed the persistence of these stable atmospheric conditions throughout the survey period (10:00-18:00 LT), characterized by weak wind speeds (generally 1-

3 m/s), absence of precipitation, and limited synoptic variability. These conditions reduced advective mixing processes that typically attenuate urban thermal contrasts, while the average measured thermal at WMO stations ranged between −3.4°C to +1.4°C, during the survey interval, favoring the preservation of local land-use-related temperature gradients (*Meteo Buzău, 10.02.2026*, 2026; *Meteo Galați, 10.02.2026*, 2026).

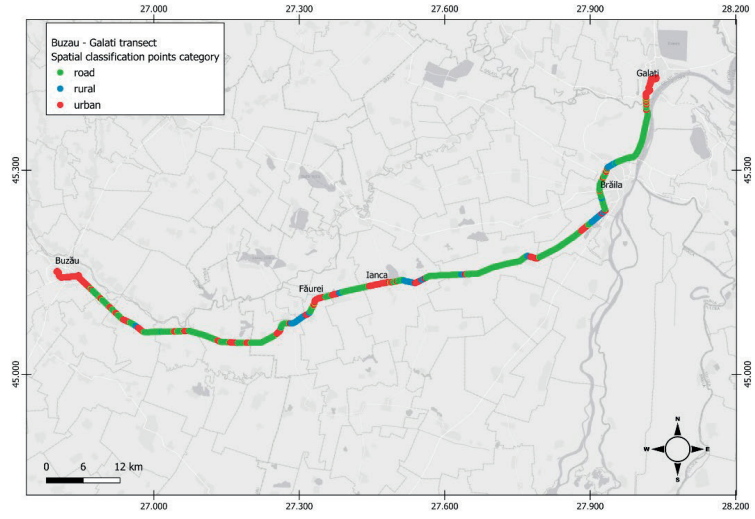
Following the quality-control and correction procedures, the mobile observations were spatially classified into three principal environmental categories: Urban, Rural, and Road environments. The classification was performed using OpenStreetMap-derived land-use and road-network information, combined with reverse geocoding and spatial proximity analysis (Boeing, 2017; *OpenStreetMap*, 2026). Urban sectors were identified based on the presence of continuous built-up areas characterized by increased building density and dominant residential, commercial, or industrial land-use classes. Rural sectors corresponded mainly to agricultural land, grasslands, open fields, and sparsely developed surfaces located outside compact settlements. Measurements situated directly along major transportation corridors or road infrastructure outside continuous urbanized areas were classified as Road environments. The spatial classification procedure enabled the differentiation and comparison of localized thermal signatures associated with urban morphology, land-use characteristics, and transportation-related environments along both regional transects.

Figure 2 presents the spatial configuration and automated environmental classification of the two mobile monitoring transects performed on 10 February 2026 between Slobozia Conachi-Buzău (Figure 2a) and Buzău-Galați (Figure 2b). The figure represents the output of a custom Python-based spatial classification workflow developed to process the corrected mobile temperature measurements. The classification algorithm automatically analysed the spatial distribution of each measurement point using land-use information, building-density characteristics, and road-network data extracted from the OpenStreetMap database (Boeing, 2017; *OpenStreetMap*, 2026). Unlike a simple administrative classification, the method was designed to identify the actual local microclimatic environment surrounding each measurement point. Thus, points located administratively inside city boundaries but lacking built-up characteristics were not automatically classified as Urban.

Urban environments were assigned only where clear built-up evidence was identified, including residential, commercial, industrial, or construction land-use polygons, the presence of at least six buildings within a 150 m radius, or a building-area ratio ≥ 0.015 within the same search distance. Rural environments corresponded mainly to agricultural and open natural surfaces, while the Road category included measurements located within 60 m of transportation corridors outside continuous built-up areas. The resulting classification highlights the strong spatial heterogeneity encountered along both regional transects, with extended Rural sectors identified between Slobozia Conachi, Focșani, and Râmnicu Sărat, as well as between Buzău, Ianca, and Brăila, whereas the largest Urban environments were associated with the metropolitan sectors of Buzău, Brăila, and Galați.



(a)



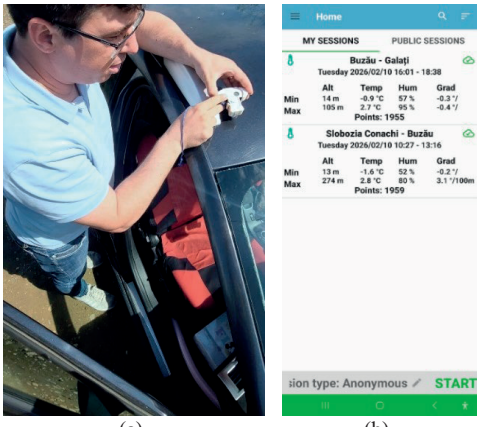
(b)

Figure 2 .Measurement track and results of spatial classification of the mobile monitoring transects from 10 February 2026 between Slobozia Conachi-Buzău (a) and Buzău-Galați (b). Red segments represent Urban environments associated with compact built-up areas and higher building density, dark blue segments indicate Rural environments dominated by agricultural and open land surfaces, while light green segments correspond to Road environments located mainly along transportation corridors outside continuous urbanized areas

Instrumentation and mobile monitoring protocol

Meteorological data were collected using the MeteoTracker (MTX-SA) standalone weather station, a device specifically engineered for high-resolution measurements on the move (MeteoTracker, 2025). The device features the patented dual-sensor Radiation Error Correction System (RECS), which dynamically corrects the "radiative error" caused by solar exposure (Jurato, J., 2020). The system ensures an air temperature accuracy of ±0.1°C (typical) and ±0.4°C under direct solar radiation at speeds exceeding 10 km/h (MeteoTracker, 2025). The performance of this sensor has been validated against reference meteorological equipment, confirming its suitability for urban microclimate investigations (Barbano et al., 2024; Loglisci et

al., 2024). During the mobile measurements performed on 10 February 2026, the device was mounted on the roof of a vehicle (see Figure 3) to minimize heat interference from the engine and asphalt, operating with a high temporal sampling resolution during the mobile survey , according to the manufacturer's specifications (Barbano et al., 2024b; Loglisci et al., 2024; MeteoTracker, 2025; Silva et al., 2025). The meteorological measurements recorded by the MeteoTracker (MTX-SA) weather station were transmitted in real time via Bluetooth to the MeteoTracker mobile application, where the data were continuously visualized and stored during the survey. Subsequently, the recorded datasets were automatically synchronized and uploaded to the MeteoTracker cloud platform, allowing remote access, download, and post-processing analysis from any location. The MeteoTracker application provides multiple visualization and statistical analysis functionalities, including real-time mapping of the measurement route with associated air temperature values, graphical representations of the recorded meteorological parameters, and the possibility to publicly share the monitoring project together with all corresponding spatial and temporal information (MeteoTracker / IoTopon Srl, 2026).



(a) (b)

Figure 3 . MeteoTracker mobile weather station mounting on the vehicle roof top during the mobile measurement campaign performed on 10 of February 2026 (a). Print screen from Meteo-Tracker app statistics data of the parameters recorded during measurements performed: Slobozia-Conachi – Buzău city and Buzău city – Galati city (b). Data Processing and Correction Procedures

Meteorological and positioning data acquired during the mobile transects conducted on 10 February 2026 were exported from the MeteoTracker+ application and subsequently processed using custom Python scripts.

The preprocessing workflow included data synchronization, quality-control procedures, filtering operations, and correction algorithms designed to remove anomalous records and improve the spatial and temporal consistency of the dataset. A three-stage quality control and normalization workflow was implemented.

The first stage aimed to prevent thermal contamination from the vehicle and surrounding traffic during stops. To this end, a speed-based filtering threshold was applied. Following the manufacturer's technical specifications and validated performance assessments, all data points recorded at speeds below 10 km/h were excluded from the final spatial analysis. This filtering ensures that the Radiation Error Correction System (RECS) operates within its optimal ventilation parameters, maintaining an accuracy of ±0.4°C even under solar exposure (MeteoTracker, 2025).

In the second stage, an altitude correction was applied to normalize the recorded air temperature (T_{obs}) to a common regional reference level (H_{ref}=50 m a.s.l.), accounting for the topographical variability of the Romanian Plain and Subcarpathian transitions areas. The corrected temperature (T_{alt_corr}) was calculated using the standard environmental lapse rate presented in the next equation:

$$T_{alt_corr} = T_{obs} + \Gamma\left(H_{obs} - H_{ref}\right) \quad (1)$$

where:

Γ is the altitudinal temperature gradient of 0.0065°C/m (or 0.65°C/100 m);

T_{obs} is the measured temperature;

H_{obs}- is the altitude of the observation point and H_{ref} – is the altitudinal average reference calculated from all measurements altitudinal level.

In the third stage, a time-drift correction was performed to isolate the spatial microclimatic signal from the natural diurnal temperature variation. Given the segmented nature of the transect and the 3-hour stationary period in Buzău, a linear interpolation was applied between the hourly observations of the ANM

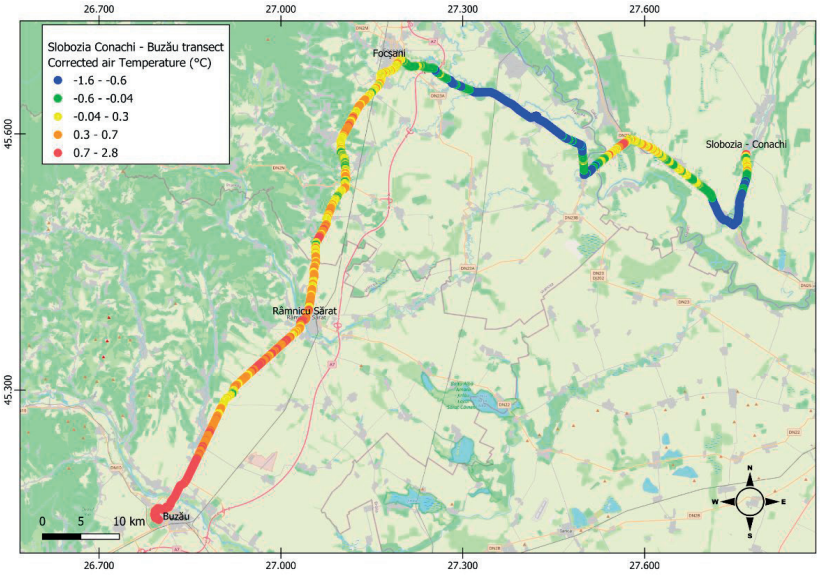
baseline stations (Galați and Buzău). This procedure adjusted each mobile observation relative to the regional heating/cooling rate of the air mass at the exact moment of sampling (data from Figure 2), ensuring that the observed gradients reflect land-use differences rather than the passage of time as stated by other studies (Chàfer et al., 2022; Kousis et al., 2022; Ichim et al., 2024). The corrected and normalized dataset obtained after the preprocessing workflow was subsequently used for the spatial classification and statistical analysis of the mobile measurements.

RESULTS AND DISCUSSIONS

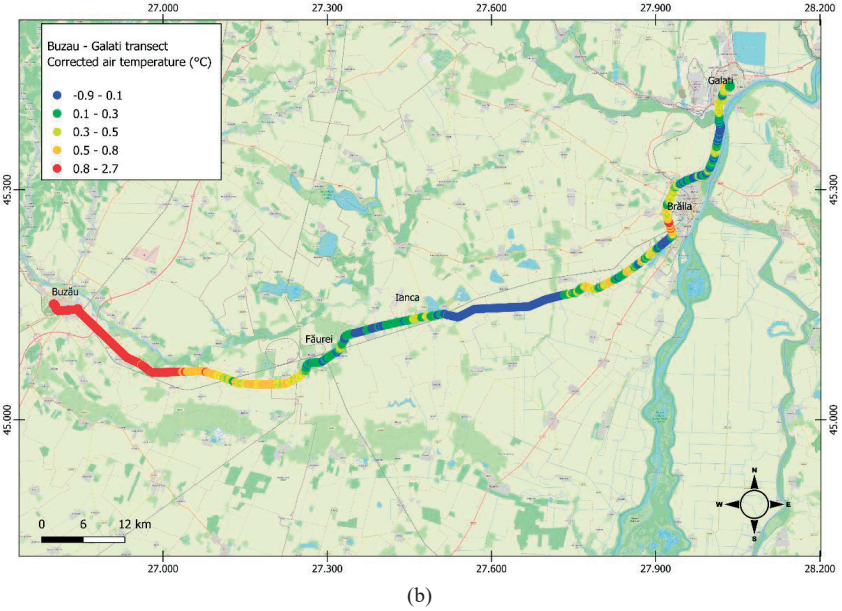
Spatial distribution of corrected air temperature

The corrected mobile measurements presented in Figure 4 represent the spatial distribution of point-based air temperature observations after the application of the filtering and correction workflow described in the methodology section. The corrected temperatures are displayed directly along the monitored routes and highlight distinct thermal contrasts associated with differences in land use, urban density, road infrastructure, and surrounding rural landscapes. Figure 4a shows the point-based spatial distribution of corrected air temperature along the Slobozia Conachi-Buzău transect after filtering and correction procedures. The coldest sectors are observed mainly in the rural area west and south-west of Slobozia Conachi and on the eastern approach toward Focșani, where several segments fall within the blue class, corresponding to corrected temperatures between −1.6 and −0.6°C. These low values are associated with open rural surfaces, agricultural land, and low building density. Around Focșani, temperatures increase mostly into the −0.04 to +0.3°C and +0.3 to +0.7°C classes, indicating a transition toward more built-up and road-influenced environments. Between Focșani and Râmnicu Sărat, the route is dominated mainly by yellow and orange classes, with corrected temperatures generally ranging from −0.04 to +0.7°C, rather than by the coldest blue values. This suggests more moderate thermal conditions along the main road corridor and nearby settlements. The warmest sector appears toward Râmnicu Sărat and especially near Buzău, where orange and red classes dominate, with corrected temperatures exceeding +0.7°C and locally reaching the highest class of the transect, up to +2.8°C. This pattern indicates stronger heat retention in compact urbanized sectors compared with the surrounding rural landscape, as it was studied in other similar studies (Barbano et al., 2024; Loglisci et al., 2024).

Figure 4b shows the point-based spatial distribution of corrected air temperature along the Buzău–Galați transect after the filtering and correction procedures. The warmest sector is clearly observed near Buzău, where the route is dominated by red points corresponding to corrected temperatures between +0.8 and +2.7°C. This indicates a strong local thermal signal associated with the compact urban area of Buzău and nearby built-up surfaces. Immediately after leaving Buzău, the route gradually shifts toward orange and yellow classes, with temperatures decreasing to +0.5–+0.8°C and +0.3–+0.5°C, reflecting the transition from urbanized land toward more open road and rural environments. The central part of the transect, especially around Făurei and Ianca, is dominated by blue and green classes, with corrected temperatures generally between −0.9 and +0.3°C. The lowest values are observed mainly along the long road corridor east of Ianca, where blue points indicate temperatures between −0.9 and +0.1°C, corresponding to open agricultural landscapes, low building density, and reduced anthropogenic heat influence. Toward Brăila, temperatures increase again, with several yellow, orange, and red segments ranging from +0.3°C to +2.7°C, consistent with the transition into a more urbanized sector. North of Brăila and toward Galați, the route alternates between colder blue-green sections and warmer yellow-orange points, indicating a mixed thermal pattern influenced by the Danube corridor, road infrastructure, and urbanized surfaces near Galați.



(a)

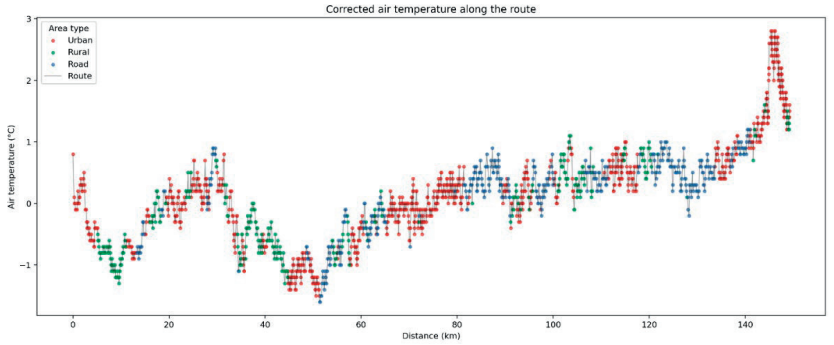


(b)

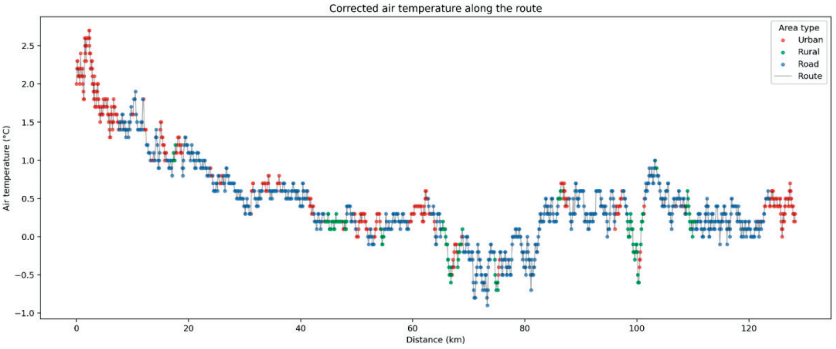
Figure 4. Spatial distribution of corrected air temperature along the Slobozia Conachi-Buzău transect (a) and the Buzău-Galați transect (b), based on mobile measurements performed on 10 February 2026. Warmer colors indicate higher corrected air temperatures, while colder colors indicate lower values

Longitudinal thermal variability along the transects

The longitudinal temperature profiles provided a detailed representation of the thermal variability recorded along the two mobile transects (Figure 5). The classification into Urban, Rural, and Road environments allowed the identification of localized thermal anomalies associated with urban morphology and transportation corridors.



(a)



(b)

Figure 5 Corrected air temperature variability along the Slobozia Conachi-Buzău transect (a) and the Buzău-Galați transect (b) classified by land-use category, based on mobile measurements performed on 10 February 2026. Red points indicate temperatures recorded within Urban sectors, green points represent Rural environments, and blue points correspond to Road-dominated areas

The longitudinal temperature profiles presented in Figure 5 reveal substantial small-scale thermal variability along both investigated transects, reflecting the strong influence of land-use characteristics and urban morphology on near-surface air temperature distribution.

Figure 5a highlights the longitudinal evolution of corrected air temperature along the Slobozia Conachi–Buzău transect, revealing a gradual transition from colder rural environments toward warmer urbanized sectors. In the first part of the route (0-15 km), corresponding mainly to rural landscapes near Slobozia Conachi, Rural measurements generally ranged between approximately −1.3°C and −0.5°C, while Road environments varied between approximately −0.9°C and −0.3°C. Between approximately 15 and 35 km, temperatures progressively increased toward positive values between approximately 0°C and +0.9°C across mixed Urban and Road sectors. The middle section of the transect (approximately 40-80 km) exhibits the coldest conditions, with several measurements below −1°C and minimum values approaching approximately −1.6°C around km 50-55. After approximately km 80, temperatures gradually increase again, while the strongest warm anomaly occurs near Buzău (approximately 140-150 km), where Urban measurements frequently exceed +2°C and locally approach +2.8°C, indicating a pronounced winter urban heat island effect.

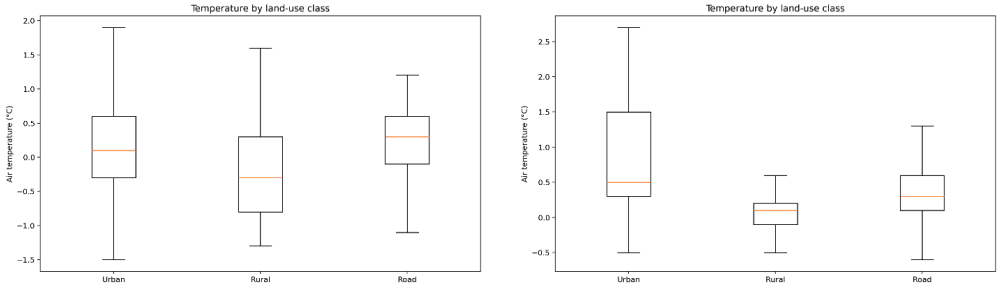
Along the Buzău-Galați transect (Figure 5b), the corrected temperature profile also reveals clear thermal contrasts between Urban, Rural, and Road environments. At the beginning of the transect (0-8 km), corresponding to the urban area of Buzău, Urban measurements remained consistently elevated, generally between +1.8°C and +2.7°C. Between approximately 10 and 40 km, temperatures progressively decreased toward less densely built and Road-dominated sectors, commonly ranging between approximately +0.3 °C and +1.2°C. The lowest

corrected temperatures were recorded in the central rural sector of the transect (approximately 55-80 km), where several measurements fall below 0°C and minimum values approach approximately −0.9°C around km 70-75. After approximately km 85, the thermal signal gradually increases again toward the Brăila-Galați metropolitan corridor, where Urban measurements remain predominantly positive, most frequently between approximately +0.5°C and +0.7°C.

Statistical analysis of data

To further evaluate the influence of land-use characteristics on local thermal conditions, the corrected air temperature values were statistically compared between Urban, Rural, and Road classes using boxplot analysis presented in Figure 6.

Figure 6 presents the boxplot distributions of corrected air temperature values for the Urban, Rural, and Road land-use categories along the two transects, providing a statistical overview of the median values, thermal dispersion, and variability ranges within each environmental class. For the Slobozia Conachi-Buzău transect (Figure 6a), the Urban category exhibits a broad thermal distribution, with values extending from approximately −1.5°C to nearly +1.9°C and a median close to +0.1°C. The central variability range (interquartile range) extends approximately between −0.3°C and +0.6°C, indicating substantial spatial heterogeneity within built-up environments. Rural sectors display lower median temperatures near −0.3°C and the coldest thermal conditions overall, with most values concentrated between approximately −0.8°C and +0.3°C. Road environments present intermediate thermal characteristics, with a median close to +0.3°C and a comparatively narrower central variability range extending approximately between −0.1°C and +0.6°C.



(a) (b)

Figure 6. Statistical distribution of corrected air temperature values for Urban, Rural, and Road environments along the Slobozia Conachi-Buzău transect (a) and the Buzău-Galați transect (b)

In the Buzău-Galați transect (Figure 6b), the Urban category again exhibits the highest positive temperatures and the widest thermal amplitude, ranging from approximately −0.5°C to +2.7°C, with a median close to +0.5°C. The central 50% of Urban temperature values are distributed approximately between +0.3°C and +1.5°C, reflecting enhanced thermal variability associated with compact built-up structures and anthropogenic heat influence. Rural environments show the narrowest thermal distribution, with a median close to +0.1°C and most values concentrated between approximately −0.1°C and +0.2°C, indicating relatively stable thermal conditions over open agricultural landscapes. Road sectors again display intermediate thermal behavior, with temperatures generally varying between approximately −0.9°C and +1.3°C and the central variability range extending approximately from +0.1°C to +0.6°C. Overall, the boxplots emphasize the stronger thermal variability and higher positive temperature anomalies associated with Urban environments, while Rural sectors remain characterized by lower and more homogeneous corrected temperature distributions along both transects.

CONCLUSIONS

This exploratory pilot study demonstrated the capability of high-resolution mobile monitoring to identify winter urban-rural thermal gradients and localized urban heat island signatures in South-Eastern Romania. The preprocessing workflow, including speed filtering, altitude normalization, temporal correction using ANM reference stations, and automated land-use classification, improved the spatial consistency and interpretability of the mobile dataset.

The results revealed clear thermal differences between Urban, Rural, and Road environments along both transects. Urban sectors, especially near Buzău and within the Brăila-Galați corridor, showed higher corrected air temperatures and greater thermal variability, while Rural areas generally maintained lower and more stable thermal conditions. Road-dominated sectors displayed intermediate thermal behavior.

Urban-rural thermal differences are not specific only to winter conditions. They can be identified throughout the year, but their intensity, spatial expression, and controlling mechanisms vary depending on season, radiation balance, wind speed, cloud cover, land cover, vegetation activity, soil moisture, and anthropogenic heat release. During winter, stable atmospheric conditions, weak wind, and reduced turbulent mixing may favor the detection of heat retention within built-up areas. In contrast, during summer, urban–rural thermal contrasts may be amplified by stronger solar radiation, reduced evapotranspiration over impervious surfaces, and the thermal behavior of construction materials compared with vegetated rural areas. Therefore, the present winter case should be interpreted as one seasonal example of urban-rural thermal differentiation, not as the only period in which such contrasts can be detected.

The combined use of point-based temperature mapping, longitudinal profiles, and boxplot statistics showed that MeteoTracker mobile measurements can capture fine-scale thermal variability that is difficult to observe using fixed meteorological stations alone. The main strength of this study lies in the high spatial resolution of the mobile observations and in the integrated workflow combining speed filtering, altitude normalization, time-drift correction, and land-use-based classification into Urban, Rural, and Road environments. This approach allowed the identification of localized winter thermal gradients and urban-rural contrasts along regional transects in South-Eastern Romania.

Although limited to a single winter day, which does not allow seasonal or climatological generalization of the observed thermal contrasts. In addition, the present analysis focused on near-surface mobile air temperature measurements and did not include satellite-derived Land Surface Temperature. Future studies should include repeated mobile surveys during different seasons and meteorological conditions and may integrate Landsat-derived LST products to compare surface thermal patterns with near-surface air temperature variability. The study confirms the usefulness of this approach for future urban climate and UHI assessments in Romania.

ACKNOWLEDGEMENTS

The authors acknowledge the support of the project An Integrated System for the Complex Environmental Research and Monitoring in the Danube River Area, REXDAN, SMIS code 127065, co-financed by the European Regional Development Fund through the Competitiveness Operational Program 2014-2020, contract no. 309/10.07.2020.

Lucian Sfîcă and Bogan Roșu contributions to this work was supported by a grant of the Ministry of Research, Innovation and Digitization, CNCS - UEFISCDI, project number PN-IV-P1-PCE-2023-0897, within PNCDI IV.

REFERENCES

Barbano, F., Brattich, E., Cintolesi, C., Ghafoor Nizamani, A., Di Sabatino, S., Milelli, M., Peerlings, E. E. M., Polder, S., Steeneveld, G.-J., & Parodi, A. (2024). Performance evaluation of MeteoTracker mobile sensor for outdoor applications. *Atmospheric Measurement Techniques*, *17*(10), 3255–3278. https://doi.org/10.5194/amt-17-3255-2024

Boeing, G. (2017). OSMnx: New methods for acquiring, constructing, analyzing, and visualizing complex street networks. *Computers, Environment and Urban Systems*, *65*, 126–139. https://doi.org/10.1016/j.compenvurbsys.2017.05.004

Brandsma, T., & Wolters, D. (2012). Measurement and Statistical Modeling of the Urban Heat Island of the City of Utrecht (the Netherlands). *Journal of Applied*

Meteorology and Climatology, *51*(6), 1046–1060. https://doi.org/10.1175/JAMC-D-11-0206.1

Chàfer, M., Tan, C. L., Cureau, R. J., Hien, W. N., Pisello, A. L., & Cabeza, L. F. (2022). Mobile measurements of microclimatic variables through the central area of Singapore: An analysis from the pedestrian perspective. *Sustainable Cities and Society*, *83*, 103986. https://doi.org/10.1016/j.scs.2022.103986

Crétat, J., Richard, Y., Pohl, B., Emery, J., Dudek, J., Roy, D., Pergaud, J., Rega, M., Poupelin, M., Joly, D., Thévenin, T., Marquès, E., & Masson, V. (2024). Impact of topography and land cover on air temperature space-time variability in an urban environment with contrasted topography (Dijon, France, 2014–2021). *Theoretical and Applied Climatology*, *155*(3), 1941–1958. https://doi.org/10.1007/s00704-023-04742-4

Eliasson, I. (1996). Urban nocturnal temperatures, street geometry and land use. *Atmospheric Environment, Conference on the Urban Thermal Environment Studies in Tohwa*, *30*(3), 379–392. https://doi.org/10.1016/1352-2310(95)00033-X

Emmanuel, R., & Krüger, E. (2012). Urban heat island and its impact on climate change resilience in a shrinking city: The case of Glasgow, UK. *Building and Environment*, *53*, 137–149. https://doi.org/10.1016/j.buildenv.2012.01.020

Hart, M. A., & Sailor, D. J. (2009). Quantifying the influence of land-use and surface characteristics on spatial variability in the urban heat island. *Theoretical and Applied Climatology*, *95*(3), 397–406. https://doi.org/10.1007/s00704-008-0017-5

Ichim, P., Miron, R., Corocăescu, A.-C., Crețu, C.-Ștefănel, & Sfîcă, L. (2024). Land use as key element for urban heat island inception in small cities. Case study: Bârlad City, Romania. *Present Environment and Sustainable Development*, *18*(1). https://doi.org/https://doi.org/10.47743/pesd2024181006

Jurato, J. G. T. (2020). *System and method for calculating the temperature of an outdoor ambient air corrected from radiation error, and sensor device usable in such system* (European Patent Office Patent No. EP3645989).

Kousis, I., Manni, M., & Pisello, A. L. (2022). Environmental mobile monitoring of urban microclimates: A review. *Renewable and Sustainable Energy Reviews*, *169*, 112847. https://doi.org/10.1016/j.rser.2022.112847

Kousis, I., Pigliautile, I., & Pisello, A. L. (2021). Intra-urban microclimate investigation in urban heat island through a novel mobile monitoring system. *Scientific Reports*, *11*(1), 9732. https://doi.org/10.1038/s41598-021-88344-y

Li, Y., Yang, T., Zhao, G., Ma, C., Yan, Y., Xu, Y., Wang, L., & Wang, L. (2024). A systematic review of studies involving canopy layer urban heat island: Monitoring and associated factors. *Ecological Indicators*, *158*, 111424. https://doi.org/10.1016/j.ecolind.2023.111424

Loglisci, N., Milelli, M., Iurato, J., Galia, T., Galizia, A., & Parodi, A. (2024). Validation of Citizen Science Meteorological Data: Can They Be Considered a Valid Help in Weather Understanding and Community Engagement? *Sensors*, *24*(14), 4598. https://doi.org/10.3390/s24144598

Martinez-Soto, A., Vera-Fonseca, M., Valenzuela-Toledo, P., Melillan-Raguileo, A., & Shupler, M. (2025). Heat on the Move: Contrasting Mobile and Fixed Insights into Temuco's Urban Heat Islands. *Sensors*, *25*(4), 1251. https://doi.org/10.3390/s25041251

Meteo Buzău, 10.02.2025. (2026, February 10). [Database]. Https://Rp5.Ru/. https://rp5.ru/Arhiva_meteo_%C3%AEn_Buz%C4%83u

Meteo Galați, 10.02.2026. (2026, February 10). [Database]. Https://Rp5.Ru/. https://rp5.ru/Arhiva_meteo_%C3%AEn_Gala%C5%A3i

MeteoTracker / IoTopon Srl. (2026). *MeteoTracker Official Platform* [App database]. MeteoTracker+. https://play.google.com/store/apps/details?id=com.iotopon.meteotracker&hl=en

MeteoTracker, I. srl. (2025). *MeteoTracker X Standalone Datasheet* [Technical datasheet]. IoTopon Srl. https://meteotracker.com/wp-content/uploads/2025/06/METEOTRACKER-X-STANDALONE-DATASHEET_rev.3.pdf

Middel, A., Häb, K., Brazel, A. J., Martin, C. A., & Guhathakurta, S. (2014). Impact of urban form and design on mid-afternoon microclimate in Phoenix Local Climate Zones. *Landscape and Urban Planning*, *122*, 16–28. https://doi.org/10.1016/j.landurbplan.2013.11.004

Oke, T. R. (1982). The energetic basis of the urban heat island. *Quarterly Journal of the Royal Meteorological Society*, *108*(455), 1–24. https://doi.org/10.1002/qj.49710845502

OpenStreetMap. (2026). [OpenStreetMap geographic database.]. OpenStreetMap Contributors. https://www.openstreetmap.org/

Romero Rodríguez, L., Sánchez Ramos, J., Sánchez de la Flor, F. J., & Álvarez Domínguez, S. (2020). Analyzing the urban heat Island: Comprehensive methodology for data gathering and optimal design of mobile transects. *Sustainable Cities and Society*, *55*, 102027. https://doi.org/10.1016/j.scs.2020.102027

Santamouris, M. (2015). Regulating the damaged thermostat of the cities—Status, impacts and mitigation challenges. *Energy and Buildings*, *91*, 43–56. https://doi.org/10.1016/j.enbuild.2015.01.027

Sfîcă, L., Crețu, C.-Ștefănel, Ichim, P., Hrițac, R., & Breabăn, I.-G. (2023). Surface urban heat island of Iași city (Romania) and its differences from *in situ* screen-level air temperature measurements. *Sustainable Cities and Society*, *94*, 104568. https://doi.org/10.1016/j.scs.2023.104568

Sfîcă, L., Ichim, P., Apostol, L., & Ursu, A. (2018). The extent and intensity of the urban heat island in Iași city, Romania. *Theoretical and Applied Climatology*, *134*(3), 777–791. https://doi.org/10.1007/s00704-017-2305-4

Silva, T., Ramusga, R., Matias, M., Amaro, J., Bonifácio, A., Reis, C., Chokhachian, A., Lopes, G., Almeida, A., Frazão, J., Vasconcelos, J., Lopes, A., & Morgado, P.

(2025). Climate walking: A comparison study of mobile weather stations and their relevance for urban planning, design, human health and well-being. *City and Environment Interactions*, *27*, 100212. https://doi.org/10.1016/j.cacint.2025.100212

Stewart, I. D., & Oke, T. R. (2012). Local Climate Zones for Urban Temperature Studies. *Bulletin of the American Meteorological Society*, *93*(12), 1879–1900. https://doi.org/10.1175/BAMS-D-11-00019.1

Voogt, J. A., & Oke, T. R. (2003). Thermal remote sensing of urban climates. *Remote Sensing of Environment, Urban Remote Sensing*, *86*(3), 370–384. https://doi.org/10.1016/S0034-4257(03)00079-8.